Digital Logic Circuit Based on a Single Molecular System of Salicylidene Schiff Base

Liyan Zhao, Dan Sui, Jia Chai, Yue Wang, and Shimei Jiang*

Key Laboratory for Supramolecular Structure and Materials of Ministry of Education, Jilin University, 2699 Qianjin Street, Changchun 130012, P. R. China

Received: April 22, 2006; In Final Form: September 28, 2006

The salicylidene Schiff base *N*-3,5-dichloro-salicylidene-(*S*)-α-phenylethylamine (**SPEA**) has been synthesized and characterized. Stimulated by one optical input (UV light) and two chemical inputs (OH^- and Zn^{2+}), **SPEA** undergoes reactions of photochemistry, deprotonation, and complexation. Tailing these reactions by means of the UV−vis absorption spectra and fluorescence spectra, two obvious optical outputs, an absorption band at 323 nm and a fluorescent emission peak at 460 nm, have been obtained. On the basis of encoding binary digits in these inputs and outputs applying positive logic conventions, one monomolecular circuit, which integrates one OR, two NOT, and four AND gates, has been achieved.

Introduction

In the process of miniaturization of electronic devices, organic molecules have played an important role in transferring, processing, and storing information in binary form.[1−6] Within the past decade, many inspirational examples of molecular logic gates (AND,[7] NOT,[8] OR,[9] XOR,[10] NOR,[11] XNOR,[12] etc.) have been reported. However, these simple logic gates must be integrated into more complex logic circuits for further application in future nanoprocessors and molecular computers. The transition from simple logic gates to complex digital circuits requires the chemical material that is able to process multiple inputs and outputs.

Some multi-input and multi-output logic circuits based on a single molecule or the combination of two molecules have been demonstrated.[13−15] Among them, the monomolecular logic circuit is very attractive since possible mutual interferences due to intermolecular interactions can be avoided, and thus, signal processing and communication would become more reliable.[16]

Until recently, the organic materials which can be used to simulate the multi-input and multi-output logic circuit at the monomolecular level are rare. Only a few molecular systems have been successfully reported, such as spiropyran[13,16] and benzylisoquinoline,[14a] and so forth.

In this paper, we selected the single molecular entity *N*-3,5-dichloro-salicylidene-(*S*)-α-phenylethylamine (**SPEA**) to mimic the monomolecular logic function. Concerning **SPEA**, the former contributions are mainly focused on its complexes. Its complex with lanthanum is a good catalyst for olefin epoxidation,[17] and its nickel complex was used to study the property of solvatochromism.[18] So far, systemic research on the property of ligand **SPEA** has not been done. In fact, its novel chemical and optical properties make it suitable to apply in a molecular logic circuit design.

The reason that **SPEA** can execute the novel logic circuit reported in this paper comes from the following chemical and optical properties. First, the phenolic group is quite sensitive to base and acid, so it is a potential candidate for a fabricating pH switch. Second, the **SPEA** is nonfluorescent, but its zinc complex displays strong fluorescence emission. So, it is a desired molecule that may form the fluorescence switch. Third, it is a photochromic molecule, which can transform from the enol form to the keto form under UV light irradiation. With these considerations in mind, we introduce the OH^-, Zn^{2+}, and UV light as the inputs; consequently, two obvious optical signals have been presented. So, a complex monomolecular logic circuit that can transduce one optical and two chemical inputs into two optical outputs has been demonstrated. This is the first report that a salicylidene Schiff base can be used for this particular kind of monomolecular logic circuit.

Experimental Section

Materials. 3,5-Dichloro-salicylaldehyde and (*S*)-α-phenylethylamine were purchased from Aldrich. The salicylidene compound **SPEA** is synthesized by the condensation of the corresponding amines with salicylaldehyde according to the standard procedures as previously reported.[19] Pure **SPEA** is obtained after recrystallization twice from absolute ethanol. The analysis data are as follows.

SPEA: ^{1}H NMR (500 MHz, $CDCl_3$, 25 °C, TMS): $\delta = 14.71$ (s, 1H), 8.28 (s, 1H), 7.40−7.14 (7H; Ar−H), 4.63 (q, ^3J (H, H) = 6.57 Hz), 1.66 (d, ^3J (H, H) = 6.69 Hz, 3H). FTIR transmission (KBr pellet): 3253 cm^{-1} (ν_{OH}), 2981 cm^{-1} (ν_{CH3}), 2771 cm^{-1} (ν_{OH}), 1629 cm^{-1} ($\nu_{C=N} + \nu_{C=C}$), 1598 cm^{-1} ($\nu_{C=C}$), 1490 cm^{-1} ($\nu_{C-O} + \nu_{C=C}$) 1450 cm^{-1} (ν_{C-N}), 1376 cm^{-1} (δ_{CH} in CH−N), 1330 cm^{-1} ($\nu_{C=C}$), 1218 cm^{-1} ($\nu_{CO} + \nu_{OH}$), 1178 cm^{-1} (ν_{C-H} in phenyl), 1126 cm^{-1} ($\nu_{C=C}$), 1029 cm^{-1} ($\nu_{C=C}$), 999 cm^{-1} ($\nu_{C=C}$). MS: $m/z = 293$ (M^+). Anal. Calcd for $C_{15}H_{13}C_{l2}NO$ (294.18): C, 61.24; H, 4.45; N, 4.76. Found: C, 61.64; H, 4.43; N, 4.47.

Experimental Details for Spectral Studies. All of the spectral analyses are accomplished in spectrograde ethanol. The concentration of **SPEA** solution for spectral analysis is 6.5×10^{-5} M. Solutions for UV−vis absorption or fluorescence spectrophotometric titration are titrated directly in 1 cm absorption cells by successive additions of corresponding chemical reagent using a microliter syringe. After addition of each aliquot, the cell is capped and mixed by inversion and the spectrum is retaken. A low-pressure mercury lamp is used as the light source for irradiation reaction.

* To whom correspondence should be addressed. E-mail: smjiang@jlu.edu.cn. Tel.: +86-431-5168474. Fax: +86-431-5193421.

10.1021/jp062476w CCC: $33.50
Published on Web 11/09/2006

Instrumentation. The UV−vis absorption spectra are taken on a Shimadzu 3100 UV−Vis−NIR recording spectrophotometer using a 3 nm slit width. The fluorescence spectra are determined with a Shimadzu RF-5301 PC spectrofluorophotometer using 3 nm input and 3 nm output width (excitation at 370 nm). ^{1}H NMR (TMS) are recorded on a Bruker UltraShield 500 MHZ spectrometer. The FTIR transmission spectrum is performed on a Bruker IFS66V FTIR spectrometer equipped with a DTGS detector for KBr pellet. Sample chamber and optics are vacuumed to eliminate carbon dioxide and water in the air. The mass spectroscopy is measured on a Finnigam TRACE-MG mass spectrometer. Elemental analyses were performed by a Perkin-Elemer PE 2400 elementar.

Quantum Yield Measurement. The quantum yield is measured at room temperature by a single excitation wavelength (370 nm, which is coming from the Xenon lamp of the spectrofluorophotometer) referenced to quinine sulfate in sulfuric acid aqueous solution ($\phi_{fr} = 0.546$) and calculated according to the eq 1,[20] where ϕ_{fs} is the radiative quantum yield of the sample; ϕ_{fr} is the radiative quantum yield of the standard; A_s and A_r are the absorbances of the sample and standard at the excitation wavelength, respectively; D_s and D_r are the integrated areas of the emission for sample and standard, respectively; L_s and L_r are the lengths of the absorption cells for the sample and standard test; and N_s and N_r are the indexes of refraction of the sample and standard solutions (pure solvents were assumed), respectively.

$$\Phi_{fs} = \Phi_{fr} \times \frac{1 - 10^{-ArLr}}{1 - 10^{-AsLs}} \times \frac{N_s^2}{N_r^2} \times \frac{D_s}{D_r} \qquad (1)$$

Results and Discussion

Absorption and Fluorescence Spectral Changes Under the Stimulations of Three Inputs.

Action of OH^- (IN1). The phenolic group is quite sensitive to bases and acids, thus when OH^- is added into the system, the deprotonation takes place immediately, so we selected OH^- as the first input signal. Continuous titration **SPEA** with NaOH induces obvious absorption spectral changes just as those shown in Figure 1a: the two original maximal absorptions at 425 nm (zwitterionic form[21,22]) and 335 nm (C═N $n-\pi^*$ transition[23−25]) gradually decrease. At the same time, a new absorption at 380 nm emerges and intensifies by degrees through two isosbestic points of $\lambda = 341.5$ and 414.5 nm, respectively. This new absorption is assigned to the deprotonation product **SPEA-1**[26] (Scheme 1). Strong changes are also observed in the emission spectra (Figure 1b) where a maximum band at 469 nm (λ_{short}) and a shoulder at 530 nm (λ_{long}) arise upon addition of NaOH. The reversibility of the deprotonation−protonation is demonstrated by the introduction of HCl into the **SPEA-1** solution. The absorption spectra shown in Figure 1a recover completely upon gradual addition of HCl (Figure S-4, Supporting Information). This circle is repeated, and the absorption intensity changes are monitored when the sample is exposed to alternating solutions of base and acid.

Action of Zn^{2+} (IN2). The salicylidene Schiff base can bind with many transition metal ions. Especially zinc complexes often display strong fluorescence emission, which can be used as a detectable output signal for molecular devices. So, we introduced the Zn^{2+} ion as the second input signal.

Complexation takes place immediately when Zn^{2+} is added into the system. Titration of **SPEA** with Zn^{2+} causes obvious changes in the absorption spectra, as shown in Figure 2a. The spectrum obtained at the end of titration compared with the

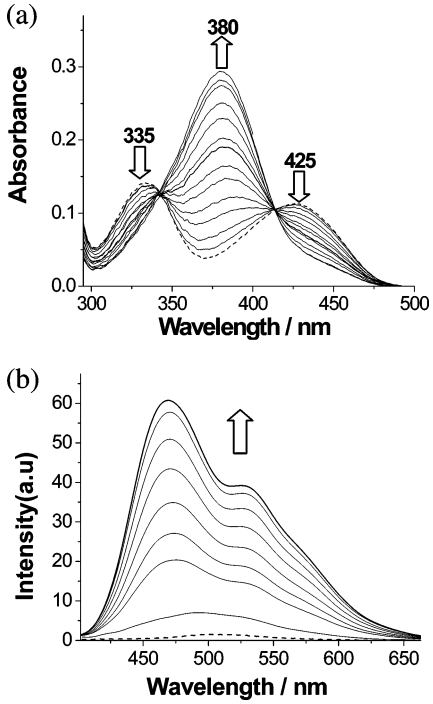

Figure 1. (a) Absorption spectra and (b) fluorescence spectra ($\lambda_{ex} =$ 370 nm) of **SPEA** before (dashed line) and after titration with NaOH (solid line).

SCHEME 1: Transitions between SPEA and SPEA-1

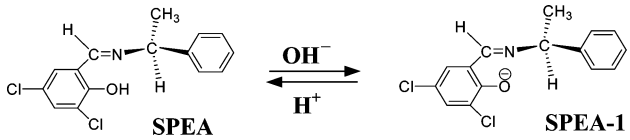

spectrum recorded before Zn^{2+} addition shows that the intensities of original peaks at 425 and 335 nm decrease and an increase takes place at the shorter 275 nm band. Four isosbestic points are observed at $\lambda = 263$, 290, 350, and 413 nm, respectively. A new broad band at 386 nm due to the N,O-complexation with Zn^{2+} develops.[26]

Plots of the decrease in absorbance at 335 nm and the increase in absorbance at 386 nm reach the saturation point when the ratio of Zn^{2+} reaches the equivalent concentration, indicating that the Zn^{2+}:**SPEA** = 1:2 (Figure 2b). The further proof for the ratio of 1:2 complexation can be achieved from the classical Job plot.[27] The Job plot (Figure 2c) shows a maximum value for the absorbance at 386 nm when the molar fraction of Zn^{2+} reaches 0.333, which is also a signature of a 1:2 binding between the ligand **SPEA** and Zn^{2+}, as shown in Scheme 2.

The emission spectrum of **SPEA** is quite sensitive to the presence of the Zn^{2+} ion. Figure 3a shows the fluorescence spectra of the spectrophotometric titration of **SPEA** with Zn^{2+}. The fluorescence intensity of **SPEA** in ethanol is very weak, but a remarkable blue emission at 460 nm is observed by adding a small amount of Zn^{2+} to the **SPEA** solution. The fluorescence intensity of this complex gradually increases until the Zn^{2+} amount reaches the complexation concentration.

To further explore the luminescent property of this complex, the fluorescence quantum yields of the **SPEA** system were recorded. From the job plot in Figure 3b, we can observe that the significant increase in fluorescence quantum yield results from the complexation with Zn^{2+}: from 0.0024 (for **SPEA**) to 0.076 (for **SPEA-2**). When the molar ratio of Zn^{2+} reaches the complexation ratio (0.333), the quantum yield has reached the highest value.

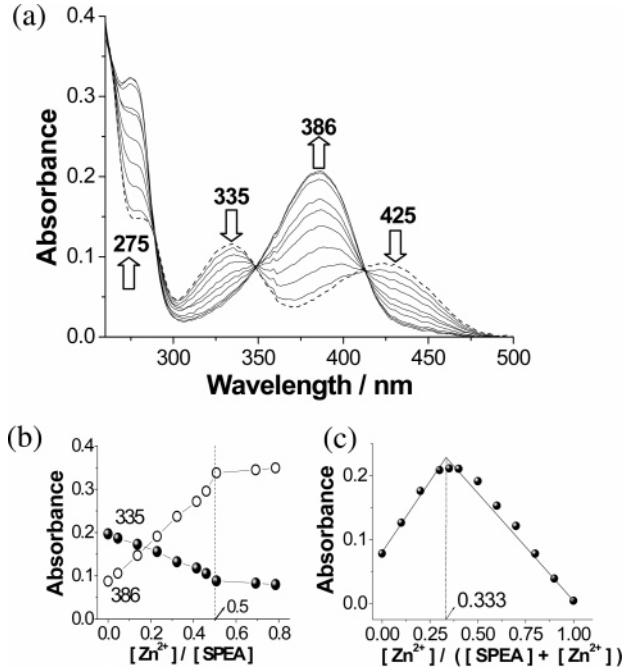

Figure 2. (a) Absorption spectral changes of **SPEA** ligand (dashed line) and upon titration with Zn^{2+} (solid line): [**SPEA**] = 6.5×10^{-5} M, [Zn^{2+}] = 0, 0.3, 0.9, 1.5, 2.1, 2.7, 3.0, 3.3, 3.9, 4.5×10^{-5} M; (b) titration profiles at 335 and 386 nm; (c) Job plot of absorbance at 386 nm and the molar fraction of Zn^{2+}.

SCHEME 2: Transitions between SPEA and SPEA-2

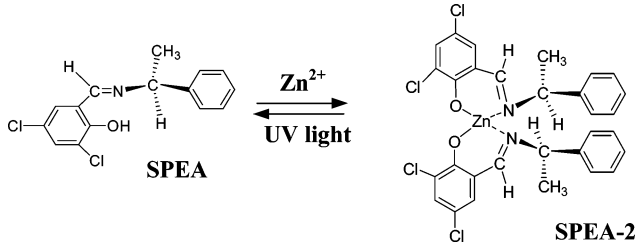

Action of UV Light (IN3). The salicylidene Schiff base is a well-known family of photochromism. So, we choose UV light as the third input signal. The studies on the photochromic trait of these Schiff base derivatives have been continued for several decades.[28] As a member of this family, **SPEA** can also respond to photic and thermic stimulations and perform the reversible reaction (Scheme 3). By irradiation with 254 nm UV light, the electronic absorption spectra of **SPEA** gradually changes (Figure 4a): the original absorption bands at 425 and 335 nm decrease along with the increase of the absorbance at 280 nm which corresponds to the keto form.[28e] These results clearly indicate that the **SPEA** has changed to the keto form **SPEA-3** under UV irradiation. This photochromism process is completed in the course of 20 min under the present experimental conditions. It should be noted that the spectral changes shown here are not obvious enough and no clear isosbestic points are observed. This is attributed to the influence of ethanol solvent. Ethanol is a strong polar solvent which will affect the proton-transfer process of photochromism. If we replace ethanol by chloroform, then immediate and progressive spectral changes with well-defined isosbestic points are observed (Figure S-5, Supporting Information). But, all of the other input stimulations are acted in ethanol solvent. To keep the stimulations being accomplished in the same environment, here we present the photochromic results in ethanol. The reversibility of the photochromism can be driven by heating (Figure S-6, Supporting Information).

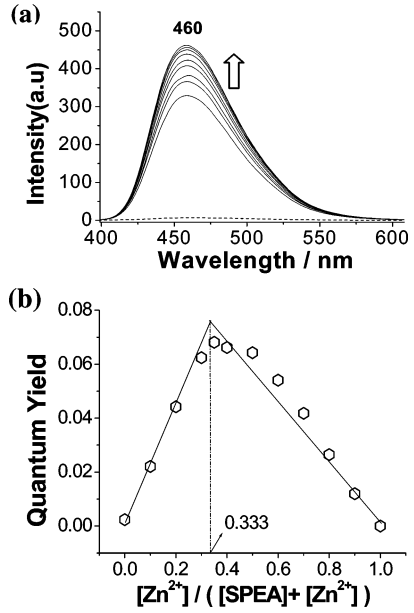

Figure 3. (a) Fluorescence spectra (λ_{ex} = 370 nm) of ligand **SPEA** (dashed line) and titration with Zn^{2+} (solid line): [**SPEA**] = 6.5×10^{-5} M, [Zn^{2+}] = 0, 0.3, 0.9, 1.5, 2.1, 2.7, 3.0, 3.3, 3.9, 4.5×10^{-5} M; (b) Job plot of the quantum yields and the molar fraction of Zn^{2+}.

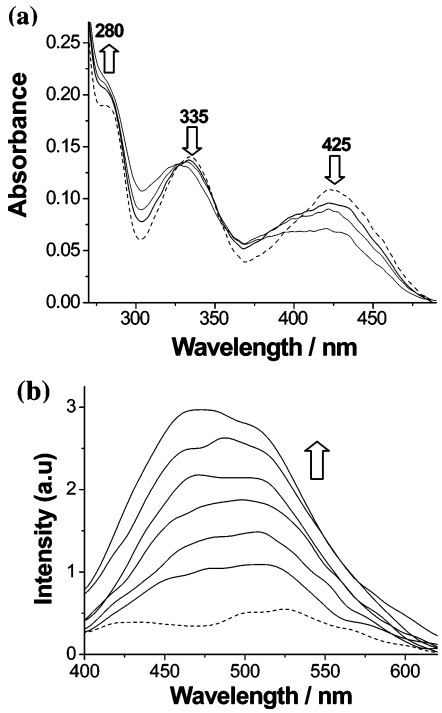

Figure 4. (a) Absorption spectra and (b) fluorescence spectra (λ_{ex} = 370 nm) of **SPEA** before (dashed line) and after continuous irradiation by 254 nm UV light (solid line).

SCHEME 3: Transitions between SPEA and SPEA-3

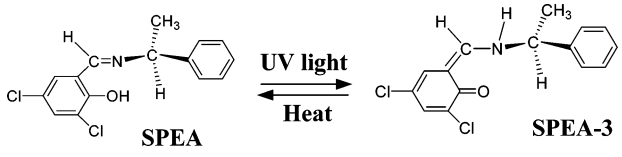

Photochromism results in fluorescent enhancements (Figure 4b). Just as reported by Barbara et al., the fluorescent emission of the salicylidene Schiff base in the enol form is very low but in the keto form the emission is stronger.[29]

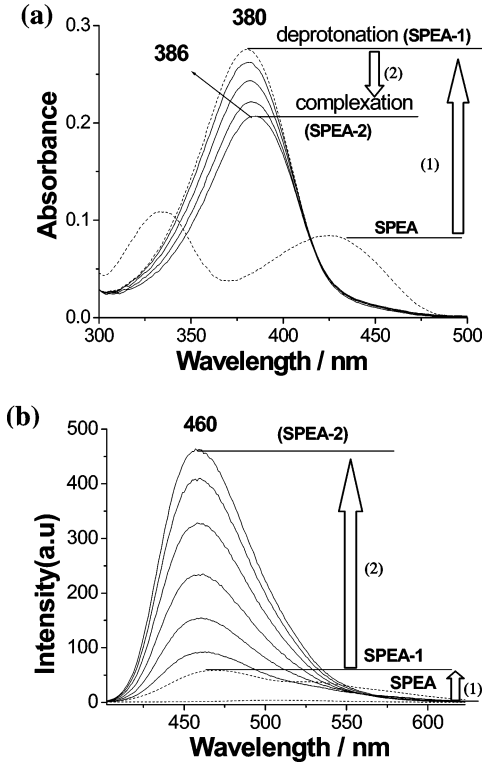

Figure 5. (a) Absorption spectra and (b) fluorescence spectra (λ_{ex} = 370 nm) of the deprotonation (step 1, dashed line) and the following complexation reactions (step 2, solid line).

Actions of OH^- and Zn^{2+} (IN1 and IN2). Now let us turn our attention to the coordinated actions of two inputs. First, by titrating **SPEA** with NaOH, as shown in Figure 5a (step 1), the typical absorption band at 380 nm emerges. This result exhibits that the ligand **SPEA** is deprotonated and transformed to **SPEA-1**. Then by titrating **SPEA-1** with Zn^{2+}, the absorption band at 380 nm decreases and is red-shifted to 386 nm (Figure 5a, step 2). As mentioned above, the band at 386 nm results from the zinc complex **SPEA-2**. So after this two-step process, we also obtain the complex **SPEA-2**.

This two-step process is further verified by fluorescent spectroscopy. As shown in Figure 5b, **SPEA** is nonfluorescent. After deprotonation, the **SPEA-1** gives a weak emission band at 469 nm. However, a significant fluorescence enhancement is produced by titrating **SPEA-1** with Zn^{2+} where a band arises at 460 nm. The intensity of such a band increases upon addition of Zn^{2+}. Finally, the intensity reaches the equivalent value shown in Figure 3a under the same excitation wavelength of 370 nm. The fluorescent spectroscopic investigation is consistent with the UV−vis spectra as mentioned above.

Actions of OH^- and UV Light (IN1 and IN3). First, by titrating **SPEA** with NaOH, we get **SPEA-1**. Then, exposure of **SPEA-1** to UV light at 254 nm leads to an unexpected absorption phenomenon, which is shown in Figure 6a. It is found that the initial absorbance at 380 nm (due to **SPEA-1**) reduces gradually along with a new absorption band centered at 323 nm which appears and increases. The absorbance between 355 and 420 nm decreases during irradiation, while the absorbance between 300 and 355 nm increases. A clear isosbestic point is found at 355 nm indicating that only two species are involved in the process. After the UV light irradiation for 20 min, the spectra will not change anymore. The new absorption band at 323 nm is blue-shifted as much as 57 nm ($\Delta\lambda_{max}$ = 380−323 nm) compared with the one at 380 nm. Such a large blue shift may be aroused from the ring-closed reaction of the deprotonated product.[30] From the corresponding fluorescence spectra (Figure 6b), we can see **SPEA** is nearly nonemissive (dashed line), but the new photoproduct displays a strong emission at 494 nm (solid line). The possible molecular structure of this new photoproduct has been presented in the Supporting Information.

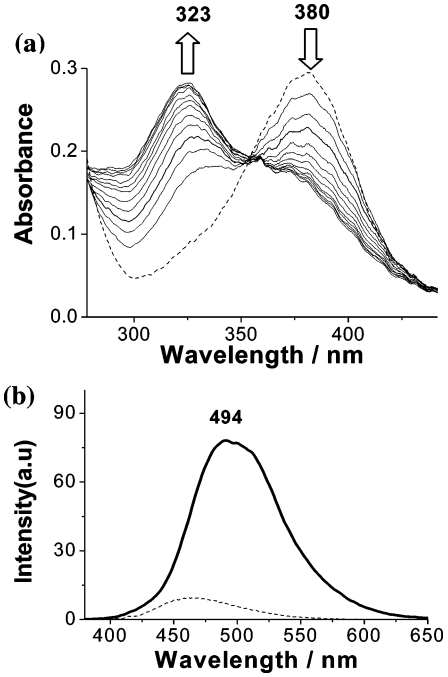

Figure 6. (a) Absorption spectra of **SPEA-1** (dashed line) and after continuous irradiation by 254 nm UV light (solid line); (b) fluorescence spectra (λ_{ex} = 370 nm) of **SPEA** solution (dashed line) and after irradiation of the **SPEA-1** by 254 nm UV light (solid line).

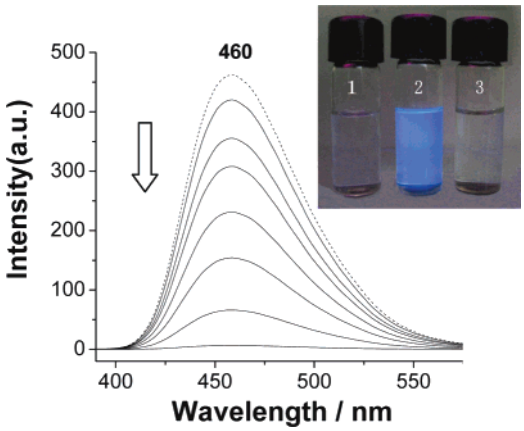

Figure 7. Fluorescence spectra of **SPEA-2** (dashed line) and after continuous irradiation by 254 nm UV light (solid line). Inset shows emission photographs in the ethanol solution: (1) the ligand **SPEA** in the absence of Zn^{2+}, (2) the Zn^{2+} complex **SPEA-2**, and (3) the **SPEA-2** after irradiated by 254 nm UV light.

Actions of Zn^{2+} and UV Light (IN2 and IN3). As mentioned above, when **SPEA** is titrated with Zn^{2+}, the complex **SPEA-2** is formed. Then we utilize the UV light to stimulate this complex. As shown in Figure 7, the intensity of the fluorescence at 460 nm (the emission of **SPEA-2)** fades gradually with irradiation by 254 nm UV light. Finally, the bright luminescence disappears when the irradiation time reaches 25 min. This result indicates that the complexation reaction can be reversed back under the UV light irradiation (Scheme 2). Additionally, this bright emission can be obtained again after it was maintained in the dark. The appearance and disappearance

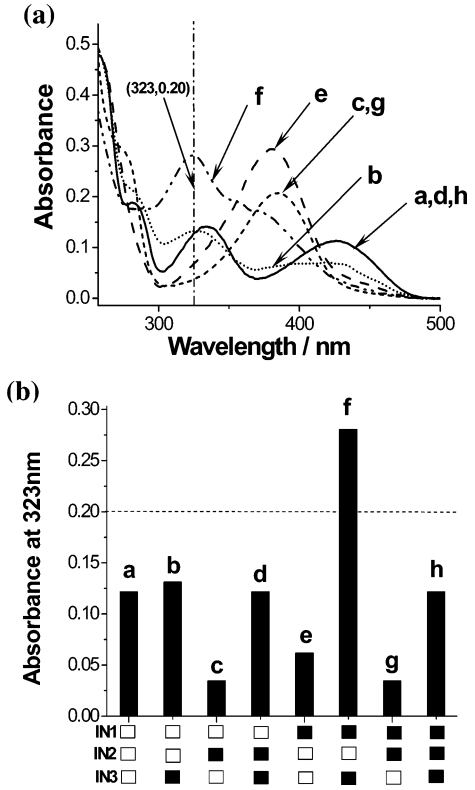

Figure 8. Under the stimulation of OH^- (IN1), Zn^{2+} (IN2), and UV light (254 nm, IN3) (IN1, IN2, IN3 in the string of a: *0 0 0*; b: *0 0 1*; c: *0 1 0*; d: *0 1 1*; e: *1 0 0*; f: *1 0 1*; g: *1 1 0*; h: *1 1 1*), (a) the absorption spectra and (b) the changes of absorbance at 323 nm (□ represents inputs that are *0*, ■ represents inputs that are *1*).

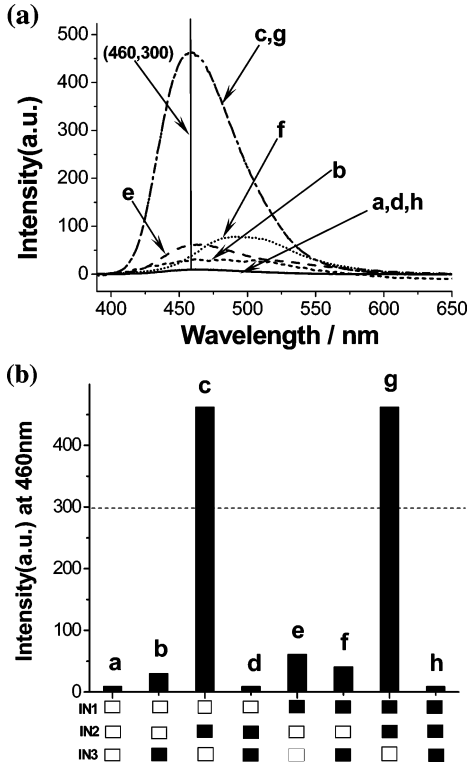

Figure 9. Under the stimulation of OH^- (IN1), Zn^{2+} (IN2), and UV light (254 nm, IN3) (IN1, IN2, IN3 in the string of a: *0 0 0*; b: *0 0 1*; c: *0 1 0*; d: *0 1 1*; e: *1 0 0*; f: *1 0 1*; g: *1 1 0*; h: *1 1 1*), (a) the fluorescence spectra (λ_{ex} = 370 nm) and (b) the changes of fluorescence intensity at 460 nm (□ represents inputs that are *0*, ■ represents inputs that are *1*).

of this characteristic fluorescence emission (at 460 nm) is convictive proof not only for its complexation reversibility but also for its switching ability as a fluorescence switch.

Actions of OH^-, Zn^{2+}, and UV Light (IN1, IN2, and IN3). Finally, we introduce all of these three inputs to **SPEA** one by one. As discussed above, by titrating **SPEA** with NaOH, we get deprotonated **SPEA-1**. Then, by titrating **SPEA-1** with Zn^{2+}, we get the **SPEA-2** complex. Next, by irradiating **SPEA-1** with 254 nm UV light, we get **SPEA** again.

In summary, under the individual actions of the OH^- ion, Zn^{2+} ion, and UV light as well as the combination of these, **SPEA** can accomplish the reactions of deprotonation, complexation, and photochemistry producing two obvious optical outputs: a UV−vis absorption band at 323 nm and a fluorescent emission peak at 460 nm.

Binary Logic Analysis for the Multi-input and Multi-output Molecular Logic Circuit. The communication between the input signals, OH^- (IN1), Zn^{2+} (IN2), and UV light (254 nm, IN3) and output signals, an absorption band at 323 nm (OUT1) and a fluorescent emission band at 460 nm (OUT2), can be described with binary logic.[31] These inputs and outputs can be encoded with binary digits applying positive logic conventions (off = *0*, on = *1*). If we regard absorbance of 0.20 and a fluorescence intensity of 300 as the threshold values, OUT1 = *0* and OUT 2 = *0* when their corresponding spectral values are lower than 0.20 and 300; OUT 1 = *1* and OUT 2 = *1* when their corresponding spectral values are higher than 0.20 and 300. Just as the spectroscopic analyses, three input stimulations will control the intensity of two output signals.

As discussed above, the absorbance at 323 nm (OUT1) is high enough only under the simultaneous actions of OH^- (IN1) and 254 nm UV light (IN3), namely, only when IN1 = *1*, IN2 = *0*, and IN3 = *1* does the output signal OUT1 = 1. Otherwise, OUT1 = *0*. The absorption spectral changes and logic properties of above reactions are shown in parts a and b of Figure 8, which demonstrate also that only when the three inputs are in the string of *1 0 1* is OUT1 higher than the threshold value (0.20).

TABLE 1: Truth Table for the Monomolecular Circuit

Input			Output	
IN1 OH^-	IN2 Zn^{2+}	IN3 *hν*	OUT1 absorption at 323 nm	OUT2 emission at 460 nm
0	0	0	0	0
0	0	1	0	0
0	1	0	0	1
0	1	1	0	0
1	0	0	0	0
1	0	1	1	0
1	1	0	0	1
1	1	1	0	0

From the spectral investigations illustrated above, the fluorescent emission band at 460 nm (OUT2) can be achieved in two situations: one is by directly titrating **SPEA** with Zn^{2+}, the other one is by titrating the deprotonated form **SPEA-1** with Zn^{2+}. In other words, only when IN1 = *0*, IN2 = *1*, and IN3 = *0* or IN1 = *1*, IN2 = *1*, and IN3 = *0* can OUT2 = *1*. The fluorescent spectral changes and logic properties of above reactions are shown in parts a and b of Figure 9 which reveal also that, when the three inputs are in the string of *0 1 0* or *1 1 0*, the fluorescent intensity at 460 nm (OUT2) is higher than the threshold value (300).

According to the two histograms (Figure 8b and Figure 9b), the truth table (Table 1) can be achieved. From which, we can see that this chemical system responds to an input string of three binary digits (IN1, IN2, IN3) producing an output string of two

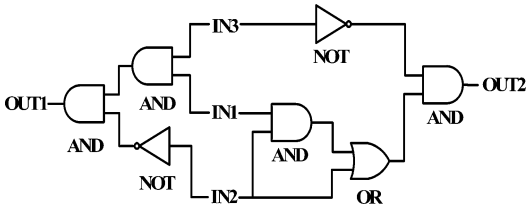

Figure 10. Combinational logic circuit equivalent to the **SPEA** molecular system.

binary digits (OUT1, OUT2). For example, the input string *0 0 0* indicates that all three input stimulations are off. Under this condition, the absorbance at 323 nm (OUT1) and the fluorescent intensity at 460 nm (OUT2) are lower than their threshold values (0.20 and 300). The output string is *0 0*. Instead, an input string of *1 1 0* indicates that the IN1 (OH^-) and IN2 (Zn^{2+}) are on but the IN3 (UV light of 254 nm) is off. Under this condition, the fluorescent intensity at 460 nm is high, while the absorbance at 323 nm is low. The output string is *0 1*. Following similar considerations, the eight output strings corresponding to the eight possible combinations of input strings can be determined. Consequently, the absorbance changes at 323 nm and the fluorescent intensity changes at 460 nm upon the external inputs of OH^- (IN1), Zn^{2+} (IN2), and UV light (254 nm, IN3) can be interpreted as a monomolecular circuit, which integrates one OR, two NOT, and four AND gates, as shown in Figure 10. One portion of the logic circuit combines the three inputs through one NOT and two AND operations producing the output OUT1. The other combines the three inputs through one NOT, one OR, and two AND operations resulting in the output OUT2. From Figure 10, we may note that the IN2 must be off when the OUT1 is on and the IN3 must be off when the OUT2 is on.

Conclusions

The salicylidene Schiff base **SPEA** is synthesized and characterized. Under the individual actions of the OH^- ion, Zn^{2+} ion, and UV light as well as the combination of these actions, we successfully obtained a multi-input and multi-output monomolecular circuit, which responds to one optical and two chemical inputs producing two optical outputs. This contribution not only develops a complex logic function based on one simple molecule by elaborate chemical design but also presents a possible material for future molecular data-processing, -storage, and -communication devices.

Acknowledgment. This work was supported by the National Natural Science Foundation of China (50573029, 50225313, and 50520130316) and the 111 Project (B06009) and Program for Changjiang Scholars and Innovative Research Team in University (PCSIRT0422).

Supporting Information Available: The ^1H NMR and FTIR spectra of **SPEA**, the stability and the further structural information about the new photoproduct, the UV−vis absorption spectra of the reversible processes of deprotonation and photochromism, and the UV−vis absorption spectra of **SPEA** photochromism in chloroform are given. This material is available free of charge via the Internet at http://pubs.acs.org.

References and Notes

(1) Amendola, V.; Fabbrizzi, L.; Mangano, C.; Pallavicini, P. *Acc. Chem. Res.* **2001**, *34*, 488−493.

(2) Raymo, F. M. *Adv. Mater.* **2002**, *14*, 401−404.

(3) Balzani, V.; Venturi, M.; Credi, A. *Molecular Devices and Machines*; Wiley-VCH: Weinheim, Germany, 2003.

(4) Badjiæ, J. D.; Balzani, V.; Credi, A.; Silvi, S.; Stoddart, J. F. *Science* **2004**, *303*, 1845−1849.

(5) Hernández, J. V.; Kay, E. R.; Leigh, D. A. *Science* **2004**, *306*, 1532−1537.

(6) Uchiyama, S.; McClean, G. D.; Iwai, K.; de Silva, A. P. *J. Am. Chem. Soc.* **2005**, *127*, 8920−8921.

(7) (a) Zhou, Y.; Zhang, D.; Zhang, Y.; Tang, Y.; Zhu, D. *J. Org. Chem.* **2005**, *70*, 6164−6170. (b) Andréasson, J.; Kodis, G.; Terazono, Y.; Liddell, P. A.; Bandyopadhyay, S.; Mitchell, R. H.; Moore, T. A.; Moore, A. L.; Gust, D. *J. Am. Chem. Soc.* **2004**, *126*, 15926−15927. (c) Callan, J. F.; de Silva, A. P.; McClenaghan, N. D. *Chem. Commun.* **2004**, 2048−2049. (d) Uchiyama, S.; Kawai, N.; de Silva, A. P.; Iwai, K. *J. Am. Chem. Soc.* **2004**, *126*, 3032−3033.

(8) (a) de Silva, A. P.; McClenaghan, N. D. *Chem.—Eur. J.* **2002**, *8*, 4935−4945. (b) Stojanovic, M. N.; Mitchell, T. E.; Stojanovic, D. *J. Am. Chem. Soc.* **2002**, *124*, 3555−3561. (c) Kolpashchikov, D. M.; Stojanovic, M. N. *J. Am. Chem. Soc.* **2005**, *127*, 11348−11351.

(9) (a) Zhan, W.; Crooks R. M. *J. Am. Chem. Soc.* **2003**, *125*, 9934−9935. (b) Ashkenasy, G.; Ghadiri, M. R. *J. Am. Chem. Soc.* **2004**, *126*, 11140−11141. (c) Guo, X.; Zhang, D.; Zhou, Y.; Zhu, D. *J. Org. Chem.* **2003**, *68*, 5681−5687.

(10) (a) Credi, A.; Balzani, V.; Langford, S. J.; Stoddart, J. F. *J. Am. Chem. Soc.* **1997**, *119*, 2679−2681. (b) Pina, F.; Melo, M. J.; Maestri, M.; Passaniti, P.; Balzani, V. *J. Am. Chem. Soc.* **2000**, *122*, 4496−4498. (c) Langford, S. J.; Yann, T. *J. Am. Chem. Soc.* **2003**, *125*, 11198−11199.

(11) (a) de Silva, A. P.; Fox, D. B.; Huxley, A. J. M.; Moody, T. S. *Coord. Chem. Rev.* **2000**, *205*, 41−57. (b) Wang, Z.; Zheng, G.; Lu, P. *Org. Lett.* **2005**, *7*, 3669−3672.

(12) (a) Asakawa, M.; Ashton, P. R.; Balzani, V.; Credi, A.; Mattersteig, G.; Matthews, O. A.; Montalti, M.; Spencer, N.; Stoddart, J. F.; Venturi, M. *Chem.—Eur. J.* **1997**, *3*, 1992−1996. (b) Bergamini, G.; Saudan, C.; Ceroni, P.; Maestri, M.; Balzani, V.; Gorka, M.; Lee, S. K.; Heyst, J. V.; Vögtle, F. *J. Am. Chem. Soc.* **2004**, *126*, 16466−16471. (c) Barragán, D.; Eu, B. C. *J. Phys. Chem. B.* **2001**, *105*, 7104−7114.

(13) (a) Raymo, F. M.; Giordani, S. *J. Am. Chem. Soc.* **2001**, *123*, 4651−4652. (b) Raymo, F. M.; Giordani, S. *J. Org. Chem.* **2003**, *68*, 4158−4169.

(14) (a) Montenegro, J. M.; Perez-Inestrosa, E.; Collado, D.; Vida, Y.; Suau, R. *Org. Lett.* **2004**, *6*, 2353−2355. (b) de Silva, A. P.; McClenaghan, N. D. *J. Am. Chem. Soc.* **2000**, *122*, 3965−3966.

(15) Andréasson, J.; Kodis, G.; Terazono, Y.; Liddell, P. A.; Bandyopadhyay, S.; Mitchell, R. H.; Moore, T. A.; Moore, A. L.; Gust, D. *J. Am. Chem. Soc.* **2004**, *126*, 15926−15927.

(16) Guo, X.; Zhang, D.; Zhang, G.; Zhu, D. *J. Phys. Chem. B* **2004**, *108*, 11942−11945.

(17) Kuhn, F. E.; Rauch, M. U.; Lobmaier, G. M.; Artus, G. R. J.; Herrmann, W. A. *Chem. Ber./Recl.* **1997**, *130*, 1427−1431.

(18) Akitsu, T.; Einaga, Y. *Polyhedron* **2005**, *24*, 1869−1877.

(19) Smith, H. E.; Cook, S. L.; Warren, M. E. *J. Org. Chem.* **1964**, *29*, 2265−2267.

(20) Demas, J. N.; Grosby, G. A. *J. Phys. Chem.* **1971**, *75*, 991−1024.

(21) Król-Starzomska; Filarowski, A.; Rospenk, M.; Koll, A. *J. Phys. Chem. A* **2004**, *108*, 2131−2138.

(22) Turbeville, W.; Dutta, P. K. *J. Phys. Chem.* **1990**, *94*, 4060−4066.

(23) Lewis, J.; W. Sandorfy, C. *Can. J. Chem.* **1982**, *60*, 1727.

(24) Jaffe, H. H.; Yeh, S. J.; Gardner, R. W. *J. Mol. Spectrosc.* **1958**, *2*, 120.

(25) Yoshida, N.; Oshio, H.; Ito, T. *J. Chem. Soc., Perkin Trans.* **2001**, *2*, 1674−1678.

(26) Yoshida, N.; Ichikawa, K.; Shiro, M. *J. Chem. Soc., Perkin Trans.* **2000**, *2*, 17−26.

(27) (a) Job, P. *Ann. Chim.* 1**928**, *9*, 113. (b) Gil, V. M. S.; Oliveira, N. C. *J. Chem. Educ.* **1990**, *67*, 473. (c) Specht, A.; Bernard, P.; Goeldner, M.; Peng, L. *Angew. Chem., Int. Ed.* **2002**, *41*, 4706. (d) Huang, F.; Gibson, H. W.; Bryant, W. S.; Nagvekar, D. S.; Fronczek, F. R. *J. Am. Chem. Soc.* **2003**, *125*, 9367−9371. (e) Huang, F.; Fronczek, F. R.; Gibson, H. W. *Chem. Commun.* **2003**, 1480.

(28) (a) Becker, R. S.; Richey, W. F. *J. Am. Chem. Soc.* **1967**, *89*, 1298−1302. (b) Moustakali-Mavridis, I.; Hadjoudis, E.; Mavridis, A. *Acta Crystallogr.,Sect. B: Struct. Crystallogr. Cryst. Chem.* **1978**, *34*, 3709. (c) Lambi, E.; Gegiou, D.; Hadjoudis, E. *J. Photochem. Photobiol. A* **1985**, *86*, 241. (d) Nakatani, K.; Delaire, J. A. *Chem. Mater.* **1997**, *9*, 2682−2684. (e) Zhao, J.; Zhao, B. *Chem. Lett.* **2000**, 268−269.

(29) Barbara, P. F.; Rentzepis, P. M.; Brus, L. E. *J. Am. Chem. Soc.* **1980**, *102*, 2786−2791

(30) Chen, Y.; Zeng, D. X. *J. Org. Chem.* **2004**, *69*, 5037−5040.

(31) Mitchell, R. J. *Microprocessor Systems: An Introduction*; Macmillan: London, 1995.